A R C H I V E O F M E C H A N I C A L E N G I N E E R I N G

VOL. LXIII 2016 Number 1

10.1515/meceng-2016-0006

**Key words:** friction, wear, PVD coated carbide, $\alpha$-$\beta$ titanium alloy

*WIT GRZESIK*, JOANNA MAŁECKA*, ZBIGNIEW ZALISZ*, KRZYSZTOF ŻAK*, PIOTR NIESŁONY**

# INVESTIGATION OF FRICTION AND WEAR MECHANISMS OF TiAlN COATED CARBIDE AGAINST Ti6Al4V TITANIUM ALLOY USING PIN-ON-DISC TRIBOMETER

The tribological behavior of the PVD-TiAlN coated carbide inserts in dry sliding against two-phase ($\alpha$-$\beta$) titanium alloy,Ti6Al4V grade, was investigated. A modified pin-on-disc device was used to conduct experiments under variable normal load and sliding speed. Scanning electron microscopy (SEM) and X-ray micro-analyses by EDS were applied for observations of wear scars and wear products. It was revealed that the increase of sliding speed contributes to decreasing the friction coefficient under a low normal force, whereas the increase of the normal loading causes the friction coefficient is less sensitive to changes in the sliding speed and its values are equal to $\mu$ = 0.26-0.34. The adhesive nature of wear along with severe abrasive action of the Ti alloy were documented.

## 1. Introduction

Titanium alloys have found a major application in the aerospace industry where they are used in manufacturing both airframes and engine components due to high specific strength, high toughness, excellent fatigue fracture and creep resistance, and superior resistance to corrosion under hot aggressive gaseous atmosphere at temperatures higher than 800°C [1, 2]. Titanium is one of the fastest growing materials, along with composites, used in aerospace applications. Among various titanium alloys applied in the aerospace industry, the Ti6Al4V, which belongs to the two-phase ($\alpha$-$\beta$) group, constitutes about 45% to 60% of the total titanium production [2]. The review of literature clearly suggests that titanium alloys, like all heat resistance super alloys

* *Opole University of Technology, Faculty of Mechanical Engineering, 45-271 Opole, P.O. Box 321, Poland; E-mails: w.grzesik@po.opole.pl; j.malecka@po.opole.pl; k.zak@po.ople.pl; p.nieslony@po.opole.pl*

(HRSAs) classified within the S-ISO group of construction materials, are considered as extremely difficult-to-machine materials with a poor machinability rate [1, 2-4]. Possible reasons for making titanium alloys difficult-to-cut are widely pointed out in the literature including Refs. [2] and [5]. In particular, they include poor thermal properties, the capacity to maintain high strength at a high temperature, chip segmentation leading to chatter, elastic deflection (springback effect) due to low elastic modulus, high work-hardening tendency, high chemical affinity with almost all cutting tool materials resulting in excessive dissolution, intensive adhesion between the tool and workpiece causing a built-up edge and tendency to ignite during dry machining. Consequently, the cutting tools made of different materials (sintered carbides, ceramics, CBN, PCD) are more prone to thermally-activated wear mechanisms such as adhesion, diffusion and chemical dissolution, although attrition also occurs. It is clear from the above-mentioned facts that tool wear and its life are the most important technological problems in titanium machining because they directly limit the material removal rate and machining costs. Nowadays, PVD-TiAlN coated cutting tools are used frequently in titanium machining due to their high hot hardness, increased wear resistance and higher chemical stability [3, 6]. They are also used in this study due to recommendations of a world-leading aircraft company.

Wear mechanisms in the machining of titanium alloys vary according to different cutting tool/workpiece material combination and predominantly depend on $\beta$-phase fraction in the titanium alloy [7, 8]. Coated carbide tools used in the machining of ($\alpha$-$\beta$) titanium alloys are subjected to high adherence of these materials on the cutting edge which result in abrasion associated with built-up edge and cratering after coating delamination. Machining of $\alpha$ and $\beta$ rich alloys shows the dominance of abrasive wear and the deformation of the cutting edge, respectively. This study is focused on the experimental documentation of the dominant wear mechanisms in the sliding coupling of a ($\alpha$-$\beta$) titanium alloy with the PVD-TiAlN coated carbide tool under sliding velocity comparable to the chip sliding speed.

Friction in the machining of aerospace materials, including the most used Ti6Al4V titanium and nickel-based Inconel 718 alloys, was assessed using different tribo-test techniques including pin-on-ring, pin-on-cylinder, pin-on-disc layouts, but predominantly pin-on-devices with or without refreshing of sliding traces [9, 10]. The evolution of apparent friction coefficient against the sliding speed and the contact pressure was investigated by Courbon *et al.* [11] for uncoated carbide pin, by Rech *et al.* [12] for TiN coated carbide and by Egana *et al.* [13] comparatively for both uncoated and TiN coated carbides. In these three similar studies using a special tribometer equipped with a piezoelectric dynamometer, thermistor and refreshing cutting tool, the

sliding velocity was ranged between 10 and 100 m/min and the maximum normal load was set at 1000 N to generate the maximum contact pressure about 1.5 GPa. Both the adhesive and mechanical (deformation) components of the friction coefficient were determined. It was found in these studies that sliding coupling of Ti6Al4V titanium and TiN coated carbide produced friction with a very low value of $\mu_{app} \approx 0.2$ at $v_s = 100$ m/min and $p_c = 1.5$ GPa. When the sliding velocity increases from 10 m/min to 100 m/min, the friction coefficient decreases from 0.3 to 0.2 [13]. The friction model for the adhesive (local) part was derived as follows [12]:

$$\mu_{ad} = 0.31 \times v_s^{-0.163}. \tag{1}$$

In this study, the tribological behaviour of the monolayer PVD-titanium aluminium nitride (TiAlN) coated P20 carbide insert (functionally the specimen in the tribo-test) in unidirectional dry sliding against a Ti6Al4V titanium counterpart (disc in the tribo-coupling) was investigated using the pin-on-disc tribometer with variable sliding speed and normal load, similar to the previous tests performed with steel and cast iron counterparts [15].

## 2. Experimental Methodology

### 2.1. Experimental set-up

In this study, PVD-TiAlN coated carbides sliding against the specially shaped disc made of Ti6Al4V titanium alloy were tested at ambient under dry friction conditions using a pin-on-disc tribo-tester equipped with motion and loading control systems and computer DAQ systems. General view of the experimental set-up is shown in Fig. 1a, whereas its functional structure including instrumentation for process measurement and control is presented in Fig. 1b. The variable contact conditions between the specimen trace and counter-specimen plain were generated by pressing the clearance face of a triangular tool insert to the convex face of the rotating steel disc, as shown in Fig. 3. As a result, the line type of contact was always kept at the beginning of the tribo-test performed.

The main functional sub-systems of the pin-on-disc tribometer shown in Fig. 1b are [14]:

a) *the control sub-system* which enables continuous variations of both mechanical – the normal load $F_n$ and kinematic – the sliding speed $v$s. parameters. The mechanical load and rotational speed were precisely stabilized by means of pneumatic and stepless power regulation systems, respectively.

b) *the measuring sub-system* which allows measuring the friction force $F_f$, the linear wear of coupling materials $\Delta l$ and the contact temperature of the specimen $T_c$. All these factors were measured and analyzed in *real-time* mode as functions of the sliding distance, $s$, or equivalently of the test time, $t$. The coefficient of sliding friction $\mu$, defined as the ratio of the variable friction force to the constant normal load (see detail $A$ in Fig. 1b), was continuously computed and recorded.

c) *DAQ module* which consists of a 16-channel A/D converter and is controlled by an original software QBTRI7TP.BAS.

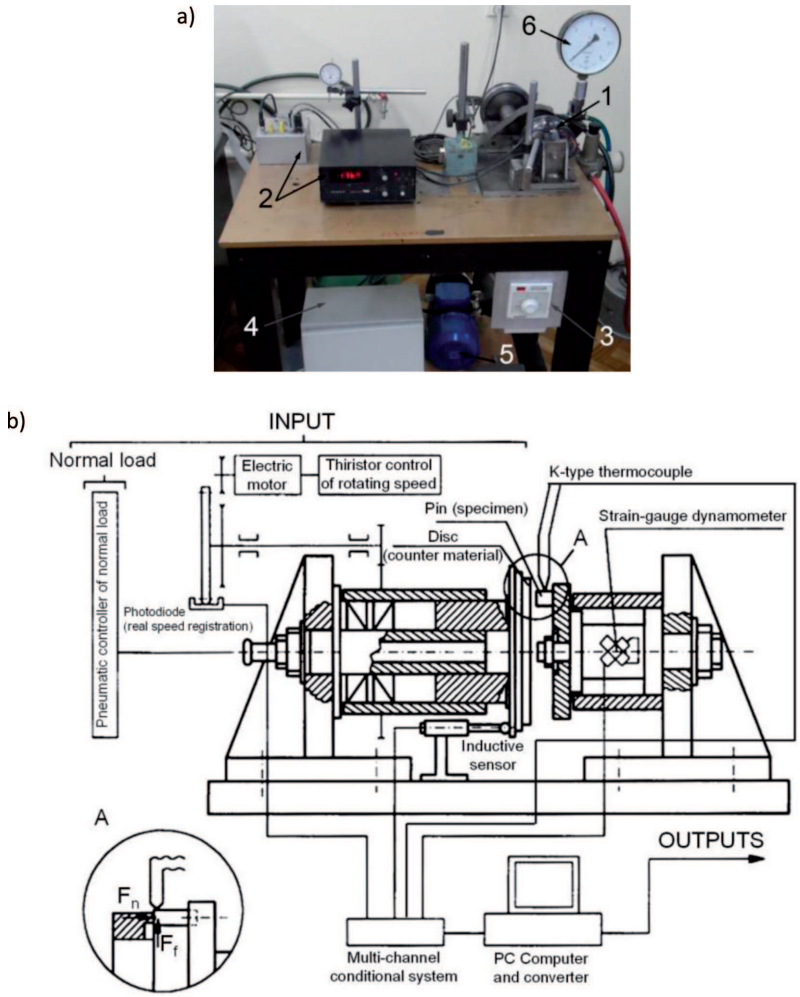


Fig. 1. View of experimental set-up (a) and structural scheme of pin-on-disc tribometer (b). 1 – pin-on-disc couple, 2 – A/C converter and signal conditioning module, 3 – temperature control panel, 4 – inverter, 5 – electrical motor, 6 – manometer

### 2.2. Coupled materials

A two-phase TiAl4V titanium alloy (UTS = 900 MPa in annealed condition), frequently used as the workpiece in metal cutting experiments of difficult-to-machine materials was selected as the counter-specimen material. As shown in Fig. 2, the face plane of the disc contains three convex traces, each of them was rounded by the radius of 1.75 mm. Titanium disc was shaped on a CNC lathe and subsequently polished to obtain the Ra roughness of about 0.2 μm to shorten the running-in period. As the specimen, commercial PVD-TiAlN ISO-P20 cemented carbide cutting insert of a CNMG120408UP rhomboidal form, KC 5010 grade by Kennametal, was used. The measured thickness of the deposited TiAlN coating was equal to 3-4 μm. According to the supplier of cutting tools tailored for high-resistance super-alloys (HRSAs) [2] this grade performs well in medium machining applications at the cutting speed of 60-90 m/min (200-300 sfm).

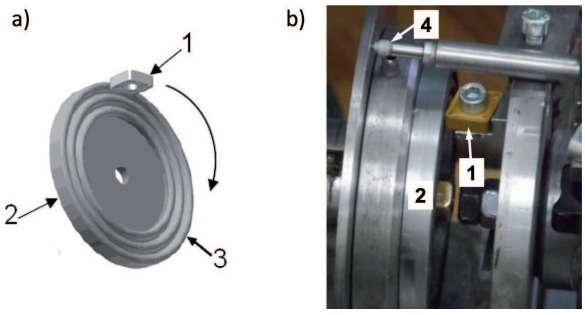


Fig. 2. Configuration of the tribo-pair tested: a) a model, b) real view. 1 – specimen, 2 – counter-specimen, 3 – convex sliding trace, 4 – inductive gauge

### 2.3. Test procedure

Sliding tribological tests were carried out with a variable normal force of $F_n$ = 10, 20 and 30 N. The sliding speed was varied from 0.5 to 1.5 m/s (three sliding speeds of $v_s$ = 30, 60, 90 m/min were selected), which corresponds to the cutting speeds normally employed when cutting titanium alloys using coated carbide tools. As a result, the matrix of experiment contains 9 different tests, i.e. at each sliding velocity with three different normal loads. The sliding distance was varied between 1000-2000 m (equivalently test time about 20-30 min). Prior to each test, the working surfaces of specimens were cleaned ultrasonically with tetrachloromethane (carbon tetrachloride) and dried in a warm air stream. Three trials were conducted for each normal load/sliding speed combination. In order to quantify the

friction behaviour of tool materials, the friction force was measured, and by using a DAQ system instantaneous values of the coefficient of friction were computed and recorded for certain intervals of time (about 4 s). Light optical microscopy (LOM) was used to examine preliminary mating surfaces and to characterize the dominant wear mechanisms of the tool materials. In this investigation, an Olympus PME3 optical microscope equipped with a JVC TK-1281 colour video camera was employed. Wear scars produced on coated inserts (specimens) were examined and identified using an HITACHI S-3400N SEM microscope equipped with an EDS THEMO NORAN System Six analyzer.

## 3. Analysis and discussion of experimental results

### 3.1. Friction coefficient

Recordings of the changes of the friction coefficient during tribo-tests obtained for three values of the normal force of 10, 20 and 30 N in the function of the sliding distance are presented in Fig. 3.

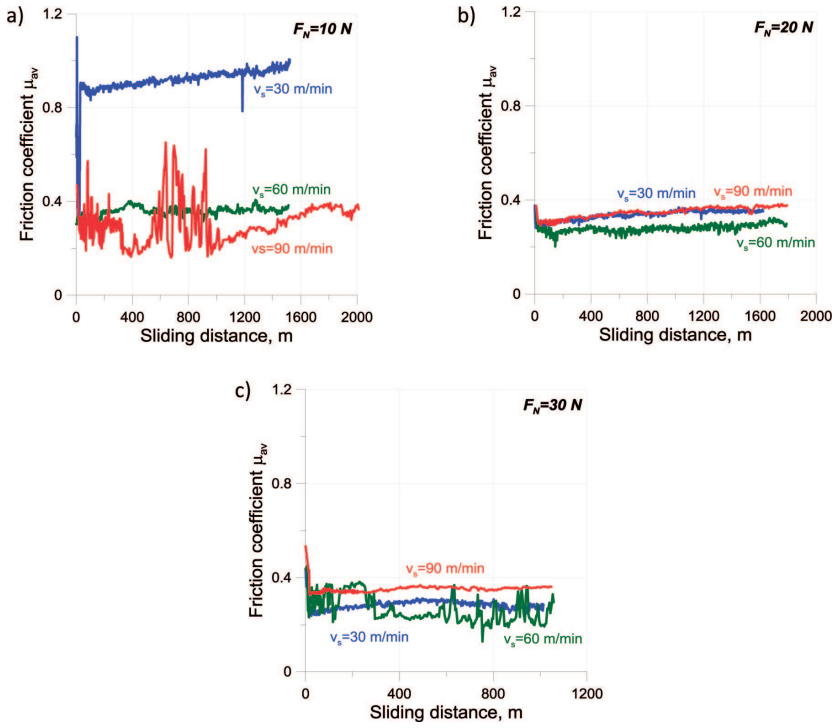


Fig. 3. Recordings of friction coefficient obtained for three normal loads applied: a) $F_N$ = 10 N; b) $F_N$ = 20 N; c) $F_N$ = 30 N

Figure 3a shows that, for the minimum normal load of $F_N$ = 10 N, the increase of the sliding velocity causes that the friction coefficient decreases substantially from 0.9–1 down to the values of 0.3-0.4. Average values of $\mu$ computed from the records shown in Fig. 3a are equal to $\mu_{av}$ = 0.89 for $v_s$ = 30 m/min, $\mu_{av}$ = 0.38 for $v_s$ = 60 m/min and $\mu_{av}$ = 0.29 for $v_s$ = 90 m/min. It can be noted that, for the minimum sliding velocity of $v_s$ = 30 m/min, the behaviour of $\mu$ is stable, whereas for the maximum sliding velocity of $v_s$ = 90 m/min visible local disturbances occur resulting from adhesive interactions between the mating surfaces (both reach of Ti) and visible chatters. During these unstable periods of tribo-test, the $\mu$ value oscillates between $0.15 < \mu < 0.65$, but for the sliding distance above 1000 m its value stabilizes at the value of $\mu_{av}$ = 0.38. For the normal loads higher than 10 N, the records of $\mu$ are relatively stable and, in general, its values do not exceed 0.4, as illustrated in Figs. 3b and c. Only for the normal load of $F_N$ = = 30 N and the sliding velocity of $v_s$ = 60 m/min some local irregularities between 0.3 and 0.4 take place. This unstable frictional behaviour of the tribo-pair is probably caused by a number of relatively large loose plasticized particles, which slide between sliding materials as illustrated in SEM images presented in Figs. 6, 8 and 10.

Figure 4 shows the calculated average values of the friction coefficient obtained according to the sliding speed for three values of the normal load selected. The values $\mu_{av}$ and their extremes (min/max) of the stored relations for the three sliding speeds are given in Table 1.

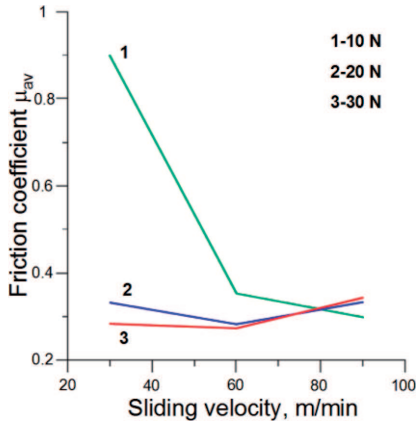


Fig. 4. Average values of friction coefficient for Ti6Al4V-TiAlN/P30 pair *vs.* sliding velocity

The data specified in Table 1 show the general trend of decreasing $\mu$ for lower normal loads and sliding speeds. The maximum value of $\mu$ was recorded for the normal load of $F_N$ = 10 N and $v_s$ = 30 m/min. For the sliding velocity above 60 m/min the $\mu$ value changes slightly and seems to

Table 1.

Selected values of $\mu_{av}$ $^{\max}_{\min}$ plotted in Fig. 4 and average friction force $F_{Tav}$ $^{\max}_{\min}$

| No. | Normal force $F_n$, N | Sliding velocity $v_s$, in m/min | Average friction coefficient $\mu_{av}$ $^{\max}_{\min}$ | Average friction force $F_{Tav}$ $^{\max}_{\min}$, N |
|---|---|---|---|---|
| 1 | 10 | 30 | **0.91** $^{\mathbf{1.10}}_{\mathbf{0.31}}$ | 9.1 $^{10.1}_{3.1}$ |
| 2 | | 60 | **0.36** $^{\mathbf{0.41}}_{\mathbf{0.29}}$ | 3.6 $^{4.1}_{2.9}$ |
| 3 | | 90 | **0.29** $^{\mathbf{0.65}}_{\mathbf{0.15}}$ | 2.9 $^{6.5}_{1.5}$ |
| 4 | 20 | 30 | **0.34** $^{\mathbf{0.38}}_{\mathbf{0.28}}$ | 6.8 $^{7.6}_{5.6}$ |
| 5 | | 60 | **0.28** $^{\mathbf{0.37}}_{\mathbf{0.21}}$ | 5.6 $^{7.4}_{4.2}$ |
| 6 | | 90 | **0.34** $^{\mathbf{0.38}}_{\mathbf{0.28}}$ | 6.8 $^{7.6}_{5.6}$ |
| 7 | 30 | 30 | **0.28** $^{\mathbf{0.44}}_{\mathbf{0.24}}$ | 8.4 $^{13.2}_{7.2}$ |
| 8 | | 60 | **0.26** $^{\mathbf{0.45}}_{\mathbf{0.13}}$ | 7.8 $^{13.5}_{3.9}$ |
| 9 | | 90 | **0.34** $^{\mathbf{0.53}}_{\mathbf{0.32}}$ | 10.2 $^{15.9}_{9.6}$ |

be independent of the normal load applied. For this range of sliding velocity, $\mu$ value varies between 0.26 and 0.34 (an apparent value of $\mu_{app}$ can be set at 0.3). This phenomenon can be explained in terms of intensive work hardening of titanium alloy observed on the worn surface. In comparison, the values of $\mu_{av}$ determined from Eqn. (1) are equal to 0.18, 0.16 and 0.15 for the sliding speeds of 30, 60 and 90 m/min, respectively, and they are underestimated in relation to the experimental data. A visible effect was that wear of the specimen increases rapidly, as depicted in Fig. 5, and by appropriate SEM images.

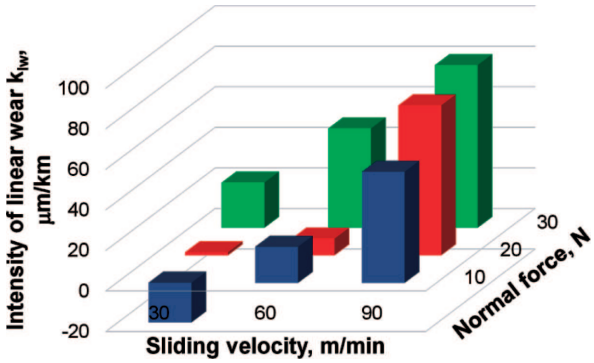


Fig. 5. Influence of normal force $F_N$ and sliding velocity $v_s$ on intensity of linear wear $k_{1w}$

As shown in Fig. 2b, a cumulated linear wear was measured by means of an inductive gauge and for the comparison of wear effects obtained for

Table 2.

Selected values of $k_{1w}$ coefficient

| Intensity of linear wear $k_{lw}$ [$\mu$m/km] for TiAlN/P20 against Ti6Al4V alloy | | | |
|---|---|---|---|
| Sliding velocity, $v_s$ / Normal force, N | 30 | 60 | 90 |
| 10 | -19.5 | 1.4 | 22.2 |
| 20 | 17.7 | 8.1 | 48.9 |
| 30 | 54.7 | 73.8 | 80.1 |

different test conditions the intensity of linear wear $k_{1w}$ was used. Its values determined for various combinations of the normal load and sliding velocity are presented in Fig. 5 and specified in Table 2. The general observation is that the $k_{1w}$ coefficient increases with the increase of the normal load for all sliding velocities applied and when sliding velocity rises itself. As reported above, some substantial differences in the changes of the relative linear wear are observed for the minimum normal load of $F_N$ = 10 N. In particular, negative linear wear (positive gauge display) was recorded for the minimum sliding velocity of $v_s$ = 30 m/min. This means that wear products are built up as the third body between the sliding surfaces as the effect of strong adhesive interaction. Apart from an intensive built-up, also the plastic flow of the adhered particles with irregular shapes and volumes takes place. This specific effect is localized along the outer boundary of the crater shown in Figs. 6b, 8b and 10b. It should be noted that such an intensive adhesion was not documented for higher values of the normal load. The maximum value of $k_{1w}$ = 80.1 μm/km was recorded for the set of $F_N$ = 30 N and $v_s$ = = 90 m/min, whereas the minimum positive one of $k_{1w}$ = 1.4 μm/km for $F_N$ = = 10 N and $v_s$ = 60 m/min respectively. The data specified in Table 2 suggests that the increase of sliding velocity causes that the adhesive bonds weaken and the predominant wear effect is due to abrasive effect. These observations of wear performance between the mating surfaces in the tribo-testing agree qualitatively with the findings in real titanium machining reported by Joshi *et al.* [3]. This wear mechanism will be discussed in detail based on SEM examinations in Section 3.2.

### 3.2. Wear identification

The wear states of worn surfaces of TiAlN coated specimens are visualized in Figs. 6, 8 and 10 for the normal loads of 10, 20 and 30 N, respectively. Moreover, for each sequence three SEM images correspond to appropriate sliding velocities of 30, 60 and 90 m/min. One SEM image was

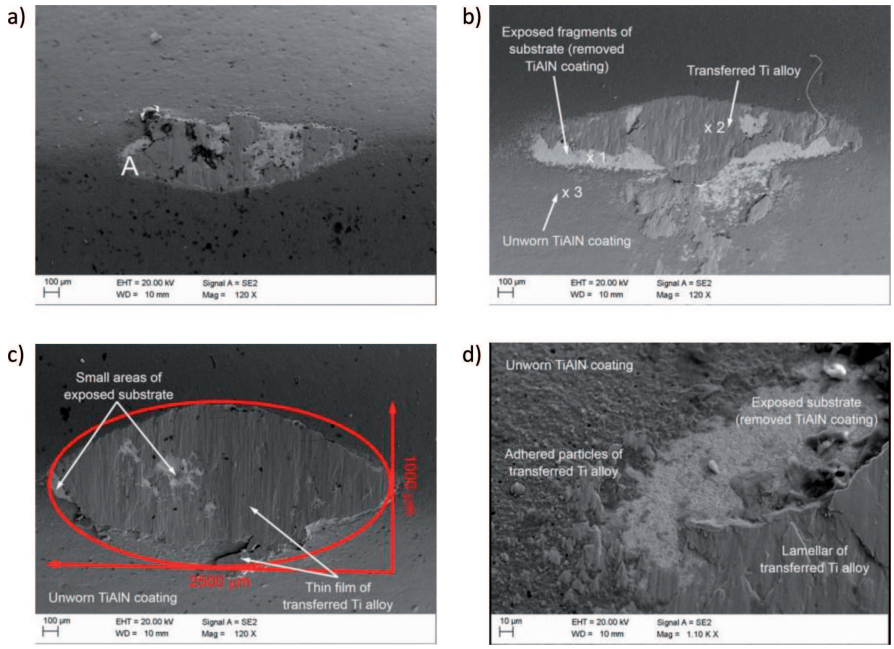


Fig. 6. SEM images of wear scatters for normal load $F_N$ = 10 N and variable sliding velocity $v_s$ = 30 m/min (a); 60 m/min (b); 90 m/min (c); magnified area A in Fig. 6a (d)

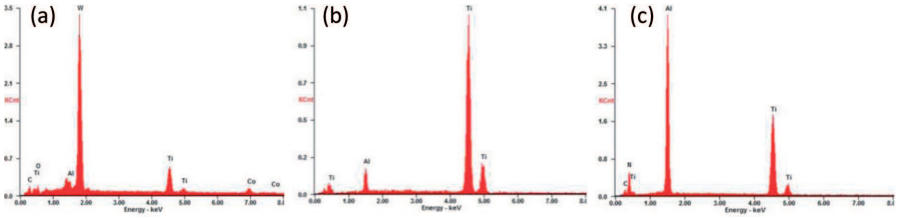


Fig. 7. EDS spectra performed at points #1 (a), #2 (b) and #3 (c) in Fig. 6b

distinctly magnified (about 10 times) in order to recognize the wear products transferred beyond the crater. EDS analysis was performed at three points 1, 2 and 3 localized in different places within the crater (point #1), in the vicinity of outer boundary of the crater (point #2) and on the coating surface near the crater (point #3). It can be generally noted based on SEM images presented in Figs. 6, 8 and 10 that wear effects are comparable for all tribological conditions. In particular, sliding interaction between the TiAlN coating and titanium alloy results in the removal of coating and forming elliptical grooves which areas depend visibly on the sliding velocity applied. For the minimum sliding velocity, the craters are more elongated in the direction of sliding movement (for instance Fig. 8a), whereas for the maximum sliding velocity the craters are less elongated in this direction (for instance Fig. 6c). It was

documented that for all case studies fragments of transferred titanium alloy are adhered to the specimen surface.

Assuming that the crater is approximately of an elliptical shape, the contact pressure was determined as the ratio of the normal load to the ellipse area, which is equal to $A_{el} = \pi ab$ where $a$ is its shorter and $b$ is its longer axis. For instance, the area of ellipse in Fig. 6c is equal to about 7.75 mm$^2$, so the contact pressure for the normal load of 10 N is equal to $p_c \approx 1.3$ MPa. At higher loads it increases to about 5 MPa.

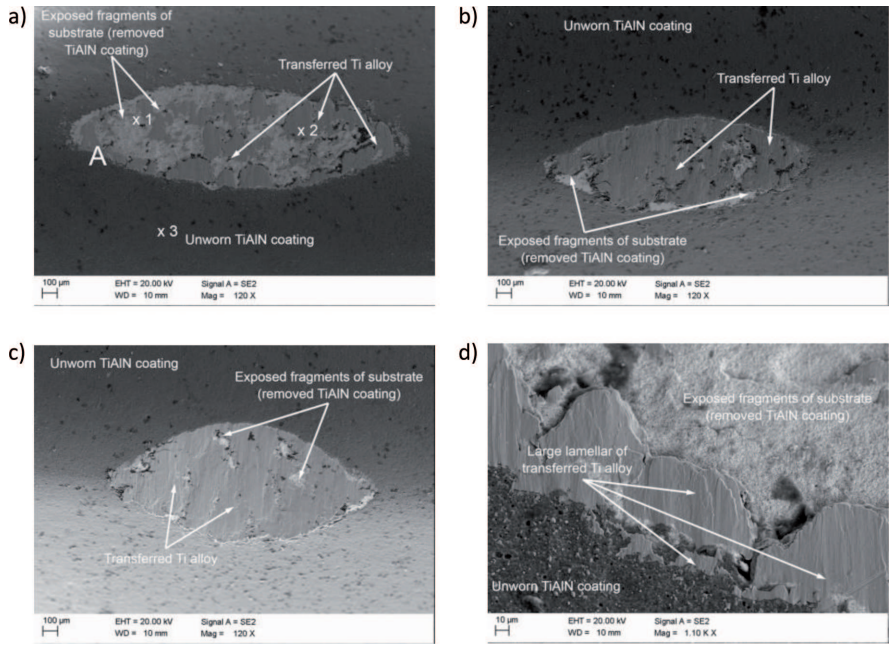


Fig. 8. SEM images of wear scatters for normal load $F_N$ = 20 N and variable sliding velocity $v_s$ = 30 m/min (a); 60 m/min (b); 90 m/min (c); magnified area A in Fig. 8a (d)

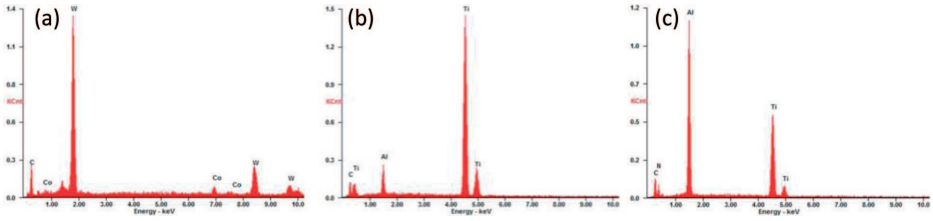


Fig. 9. EDS spectra performed at points #1 (a), #2 (b) and #3 (c) in Fig. 8b

It was found based on EDS spectra presented accordingly to SEM images in Figs. 7, 9 and 11 that sliding interactions between coupled materials of tribo-pairs result in their transfer and deposition within the contact area. In particular, massive build-ups formed from titanium alloy are produced

(see for instance Figs. 8d and 10d), which suggest strong adhesive wear mode when using TiAlN coated carbide tools in the machining of Ti6Al4V titanium alloy. All EDS spectra made at point #2 indicate a large amount of titanium depicted by two peaks of Ti easily observed in Fig. 7b (86.27%Ti), Fig. 9b (89.04%Ti) and Fig. 11b (90.56%at Ti). The deposited TiAlN coating is successively removed by abrasive action of superficially hardened titanium alloy, as depicted by points #1 in Figs. 6b, 8a and 10a. All EDS spectra made at point #1 indicate predominant amount of wolfram content (78.06 at% W – Fig. 7a; 89.62 at% – Fig. 9a; 79.12 at% – Fig. 11a) accompanied by cobalt (5.96 at% Co – Fig 7a; 6.58 at% Co – Fig. 9a; 6.01 at% Co) characteristic for the WC substrate.

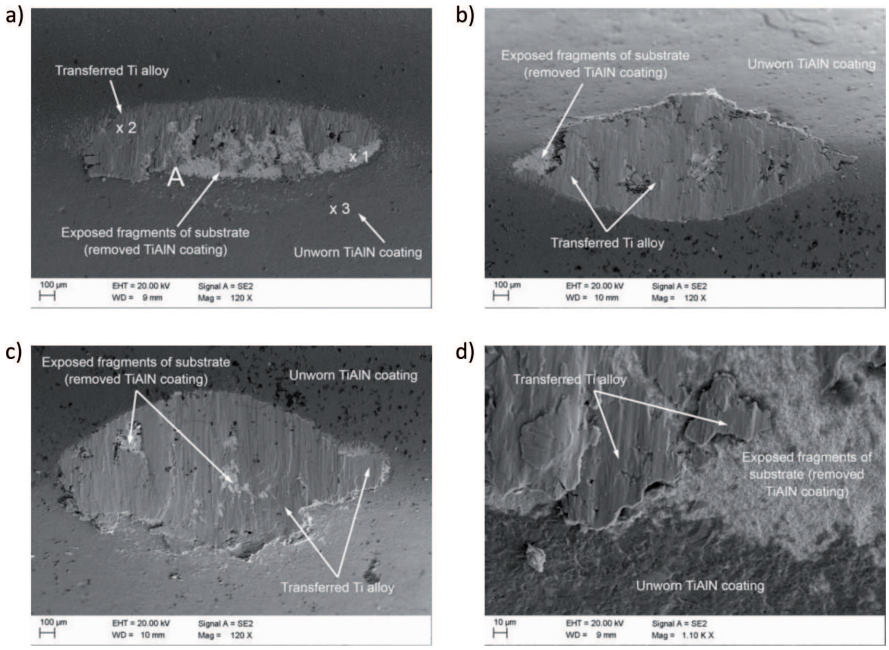


Fig. 10. SEM images of wear scatters for normal load $F_N$ = 30 N and variable sliding velocity $v_s$ = 30 m/min (a); 60 m/min (b); 90 m/min (c); magnified area A in Fig. 10a (d)

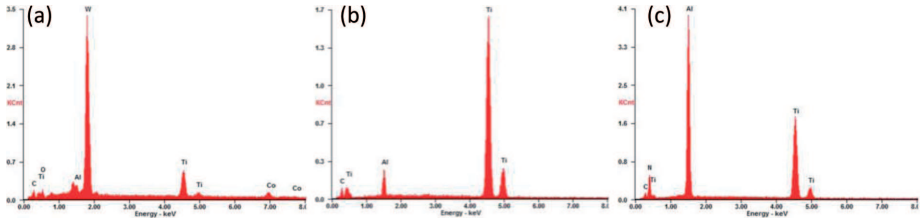


Fig. 11. EDS spectra performed at points #1 (a), #2 (b) and #3 (c) in Fig. 10b

A number of adhesive bonds with transferred titanium alloy in the form of loose particles and smeared lamellae resulting from spalling and thin interrupted layer are denoted by point #2 in Figs. 6b, 8a and 10a. The amount of the transferred titanium alloy increases substantially with the increase of the sliding velocity.

## 4. Conclusions

The following original results were specified from this study:

1. Wear intensity of the TiAlN/P20 specimen increases with the increase of both normal load and sliding velocity between specimen and counter-specimen.
2. In this study, the maximum and minimum values of friction coefficient recorded are equal to 0.26 and 0.91. The maximum $\mu$ value of 0.91 was incidentally obtained for exceptionally low load and sliding velocity.
3. The representative values of average $\mu_{av}$ = 0.26-0.36 seem to be independent of the sliding velocity in the range of $v_s$ = 30-90 m/min and the normal load in the range of 10-30 N. As a result, the average value of $\mu$ for practical purposes including analytical and FEM modelling can be preliminarily set at 0.3.
4. The predominant wear mechanisms occurring during sliding of the TiAlN/P20 insert against Ti6Al4V titanium alloy of ($\alpha$-$\beta$) structure are abrasion and adhesion. The first one causes that the TiAlN coating is removed and the crater is continuously grown, the second one results in forming large titanium build-ups on the specimen surface.
5. The average contact pressure determined by means of dimensioning of the crater area is equal to 0.13-0.5 GPa depending on the normal load exerted, which correspond to the contact pressure occurring at the secondary shear zone in metal cutting [15]. This is a crucial argument for tribo-testing as the practical method of identification of friction and wear mechanisms.

## Acknowledgments

This investigations have been carried out as part of the project No. PBS1-178595 funded by the Polish National Center for Research and Development (NCBiR).

Manuscript received by Editorial Board, September 11, 2015;
final version, February 05, 2016.

REFERENCES

[1] Grzesik W.: Advanced Machining Processes of Metallic Materials. Elsevier, Amsterdam; 2008.
[2] Yang X. Liu C.R.: Machining Titanium and its Alloys. Machining Science and Technology 1999, 3(1), pp. 107-139.
[3] High-temperature machining guide. www.kennametal.com.
[4] Ulutan U., Ozel T.: Machining Induced Surface Integrity in Titanium and Nickel Alloys: A Review. International Journal of Machine Tools and Manufacture, 2011, 51, pp. 250-280.
[5] Pramanik A.: Problems and Solutions in Machining of Titanium Alloys. International Journal of Advance Manufacturing Technology, 2014, 70, pp. 919-928.
[6] Andriya N., Rao P.V., Ghosh S.: Dry Machining of Ti-6Al-4V using PVD Coated TiAlN Tools. Proceedings of the World Congress on Engineering, WCE 2012, London, 2012: Vol. III.
[7] Joshi S., Pawar P., Tewari A., Joshi S.S.: Tool Wear Mechanism in Machining of Three Titanium Alloys with Increasing $\beta$-phase fraction. Institution of Mechanical Engineers Part B: Journal of Engineering Manufacture, 2014, 228(9), pp. 1090-1103.
[8] Pawar P., Joshi S., Tewari A., Joshi S.S.: Tool Wear Mechanisms in Machining of Titanium Alloys. Proceedings of $4^{th}$ International & $25^{th}$ AIMTDR Conference, Kolkata 2012, pp. 345-348.
[9] Grzesik W., Zalisz Z., Nieslony P.: Friction and Wear Testing of Multilayer Coatings on Carbide Substrates for Dry Machining Applications. Surface and Coatings Technology, 2002, 155, pp. 37-45.
[10] Zemzeni F., Rech J., Ben Salem W., Dogui A., Kapsa P.: Identification of a Friction Model at Tool/Chip/Workpiece Interface in Dry Machining of AISI4142 treated steels. Journal of Materials Processing Technology, 2009, 209, pp. 3978-3990.
[11] Courbon C., Pusavec F., Dumont F., Rech J., Kopac J.: Tribological Behaviour of Ti6Al4V and Inconel 718 under Dry and Cryogenic conditions – Applications to the Context of Machining with Carbide Tools. Tribology International, 2013, 66, pp. 72-82.
[12] Rech J., Arrazola P.J., Claudin C., Courbon C., Pusavec F., Kopac J.: Characterisation of Friction and Heat Partition Coefficients at the Tool-Work Material Interface in Cutting. CIRP Annals- Manufacturing Technology 2013, 62(1): 79-82.
[13] Egana A., Rech J., Arrazola P.J.: Characterization of Friction and Heat Partition Coefficients during Machining of a TiAl6V4 Titanium Alloy and a Cemented Carbide, Tribology Transactions, 2012, 55, pp. 665-676.
[14] Grzesik W., Zalisz Z., Krol S., Nieslony P.: Investigations on Friction and Wear Mechanisms of the PVD-TiAlN coated Carbide in Dry Sliding against Steels and Cast Iron. Wear, 2006, 261, pp. 1191-1200.
[15] Grzesik W.: The Influence of Thin Hard Coatings on Frictional Behaviour in the Orthogonal Cutting Process. Tribology International, 2000, 33, pp. 131-140.

**Badanie mechanizmów tarcia i zużycia węglika spiekanego z powłoką TiAlN w parze ze stopem tytanu Ti6Al4V za pomocą tribometru pin-on-disc**

Streszczenie

W artykule przestawiono wyniki badań dotyczące tribologicznego zachowania się płytek skrawających z węglika spiekanego pokrytego powłoką TiAlN w skojarzeniu z dwufazowym ($\alpha$-$\beta$)

stopem tytanu Ti6Al4V w warunkach tarcia suchego. W badaniach użyto zmodyfikowane urządzenie typu pin-on-disc, które umożliwia przeprowadzenie badań eksperymentalnych ze zmiennym obciążeniem normalnym i zmienną prędkością poślizgu. Do obserwacji śladów i produktów zużycia zastosowano mikroskopię skaningową (SEM) i mikroanalizę rentgenowską (EDS). Wykazano, że wzrost prędkości poślizgu przyczynia się do zmniejszenia współczynnika tarcia, jeśli stosuje się małe siły normalne, natomiast wzrost obciążenia normalnego powoduje, że współczynnika tarcia jest mniej wrażliwy na zmiany prędkości poślizgu i jego wartości wynoszą $\mu$ = 0,26-0,34. Udokumentowano adhezyjny mechanizm zużycia łącznie z silnym oddziaływanie ściernym stopu tytanu.